Pis'ma v ZhETF, vol. 98, iss. 9, pp. 631 – 636

Selfconsistent calculation of phonon gyromagnetic ratios in ^{208}Pb

E. E. Saperstein[+1)], *S. P. Kamerdzhiev*[*], *S. Krewald*[×], *J. Speth*[×], *S. V. Tolokonnikov*[+°]

[+]*National Research Centre "Kurchatov Institute", 123182 Moscow, Russia*

[*]*Institute for Physics and Power Engineering, 249033 Obninsk, Russia*

[×]*Institut für Kernphysik, Forschungszentrum Jülich, D-52425 Jülich, Germany*

[°]*Moscow Institute of Physics and Technology, 141700 Dolgoprudny, Russia*

Submitted 23 August 2013

Within the Theory of Finite Fermi systems the gyromagnetic ratios g_L^{ph} of all low-lying phonons in ^{208}Pb are calculated. The input data, i.e. single-particle energies, single-particle wave functions, and the ph-interaction are derived from the Energy Density Functional by Fayans et al. For the 3_1^- phonon which is the most collective state, the g_L^{ph} value is close to the prediction of the collective Bohr–Mottelson (BM) model. Gyromagnetic ratios of other phonons that are included in our calculations, two 5^- states and six positive parity phonons, differ significantly from the BM model prediction.

DOI: 10.7868/S0370274X13210091

Recently, a large amount of new data on magnetic and quadrupole moments have been obtained from the modern Radioactive Ion Beam facilities. They include nuclei as well as distant from the beta-decay valley and often close to the drip-lines. The bulk of the data is collected in a very comprehensive compilation by Stone [1]. More recent data are presented in original articles, e.g. in Ref. [2]. Here recent data on magnetic and quadrupole moments of a long chain of copper isotopes are presented and successfully described within the Many-Particle Shell Model (MPSM) [3]. This approach takes into account all main inter-nuclear correlations. However, the necessity to introduce many parameters for the effective interaction, the single-particle mean field and the effective particle charges is a severe deficiency of the MPSM. In addition, the domain of the MPSM applications is, by technical reasons, limited to nuclei with $A < 90-100$.

For heavier nuclei, the challenge of experimentalists was partially responded within the self-consistent Theory of Finite Fermi Systems (TFFS) [4–6] for magnetic moments [7, 8] and quadrupole moments [9–11] of odd spherical nuclei. We mention also the first self-consistent calculation of the quadrupole moments of the 2_1^+ states [12]. The calculations were mainly restricted to semi-magic nuclei considered in the "single-quasiparticle approximation" where one quasiparticle in the fixed state $\lambda = (n, l, j, m) = (\nu, m)$ with the energy ε_λ is added to the even-even core. The QRPA-like TFFS equations for the nuclear response to the external field, magnetic in [7, 8] or quadrupole in [9–11], were solved on the base of the Energy Density Functional (EDF) by Fayans et al. [13–15]. This version of the EDF method can be interpreted as a kind of the realization of the self-consistent TFFS [6]. For magnetic moments, the original Fayans functional DF3 [14, 15] was used whereas for quadrupole moments it was used together with its modification, DF3-a, which was introduced in [16] to extend this approach to nuclei heavier than lead. It differs from the original one by the spin-orbit and effective tensor terms which are important only for the fine structure of the single-particle spectrum in the vicinity of Fermi surface. For the quadrupole moments, the difference between the predictions of the two functionals turned out noticeable with a preference to DF3-a. The same is true for the energies and excitation probabilities of the 2_1^+ states in the lead, tin and nickel isotopes [9, 17].

On the average, reasonable description of the data was obtained in the Refs. cited above, with the accuracy of $\delta\mu \simeq (0.1-0.2)\mu_N$ for magnetic moments, and $\delta Q \simeq (0.1-0.2)$b for quadrupole moments. This indicates that generally the single-quasiparticle approximation is valid for such nuclei. However, there are several cases, with $\delta\mu \simeq 0.5\mu_N$ for magnetic moments, and $\delta Q \simeq 0.5$ b for quadrupole moments which can be attributed to phonon coupling (PC) effects. The estimations in [8] for magnetic moments and in [10] for quadrupole ones have shown that this interpretation looks reasonable and a more detailed analysis of the PC effects is necessary. Dealing with PC corrections

[1)]e-mail: saper@mbslab.kiae.ru

to magnetic moments [18, 19], one needs to know the magnetic moments or the gyromagnetic ratios g_L^{ph} for each L-phonon under consideration. Usually the prescription of the collective Bohr–Mottelson model [20], $g_{L,\mathrm{BM}}^{ph} = Z/A$, is used, see e.g. [21]. In this letter, we present results of the microscopic calculation, within the self-consistent TFFS, of this quantity for nine low-lying L-phonons in the double-magic ^{208}Pb nucleus, the standard benchmark of the nuclear theory.

The diagrams for the magnetic moment of the L-phonon are displayed in Fig. 1. The main ingredients of

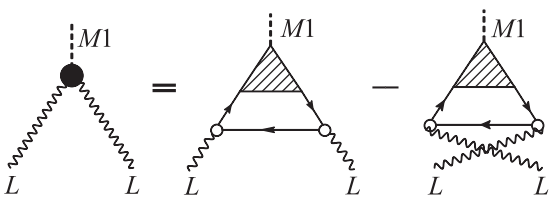

Fig. 1. Diagrams for the L-phonon magnetic moment in magic nuclei. The dashed triangle is the effective field V of the $M1$ symmetry and the open blob is the vertex g_L for creating the L-phonon

these diagrams, the effective field V and the vertex g_L obey the usual TFFS equations [4]. The first one reads:

$$V = e_q V_0 + \mathcal{F} A(\omega = 0) V, \tag{1}$$

where V_0 is the external field, $e_q[V_0]$ is the corresponding local charge, $\mathcal{F}$ is the Landau–Migdal (LM) interaction amplitude, and $A(\omega) = \int G(\varepsilon) G(\varepsilon + \omega) d\varepsilon/(2\pi i)$ stands for the particle-hole propagator, with $G(\varepsilon)$ being the single-particle Green function. The symbolic product, as usual, means the integration over intermediate coordinates and summation over the spin and isospin variables. For the problem under consideration, the external field is

$$V_0 = \hat{\boldsymbol{\mu}} = g_l \hat{\mathbf{l}} + \frac{1}{2} g_s \hat{\boldsymbol{\sigma}}, \tag{2}$$

with $g_l^p = 1$, $g_l^n = 0$, $g_s^p = 5.586$, and $g_s^n = -3.826$. For the local charge, in accordance with [7, 8], we add to the standard TFFS spin and orbital parameters ζ_s, ζ_l [4] a new "tensor" (or "l-forbidden") charge ζ_t.

The vertex g_L obeys the homogeneous equation corresponding to Eq. (1),

$$g_L(\omega) = \mathcal{F} A(\omega) g_L(\omega), \tag{3}$$

and is normalized as follows [4],

$$\left(g_L^+ \frac{dA}{d\omega} g_L \right)_{\omega = \omega_L} = -1. \tag{4}$$

For $M1$ symmetry of the effective field, the spin-dependent LM amplitude enters Eq. (1):

$$\mathcal{F}^{\mathrm{spin}} = \mathcal{F}_0^{\mathrm{spin}} + \mathcal{F}_\pi + \mathcal{F}_\rho, \tag{5}$$

where the pion and ρ-meson exchange terms are added to the central force term $\mathcal{F}_0^{\mathrm{spin}}$. Eq. (1) and all equations below were solved in the self-consistent basis $\{\lambda\}$ generated with the Generalized EDF by Fayans et al.,

$$E_0 = \int \mathcal{E}[\rho(\mathbf{r}), \eta(\mathbf{r}),] d^3 r, \tag{6}$$

depending simultaneously on the normal ρ and anomalous η densities. In the magic nucleus ^{208}Pb pairing is absent and $\eta = 0$. The DF3-a version of the normal EDF [16] is used.

All the low-lying phonons we consider have natural parity. In this case, the vertex g_L possesses even T-parity. It is the sum of two components with spins $S = 0$ and 1, respectively:

$$g_L = g_{L0}(r) T_{LL0}(\mathbf{n}, \alpha) + g_{L1}(r) T_{LL1}(\mathbf{n}, \alpha), \tag{7}$$

where T_{JLS} stand for the usual spin-angular tensor operators [22]. The operators T_{LL0} and T_{LL1} have opposite T-parities, hence the spin component should be an odd function of the excitation energy, $g_{L1} \propto \omega_L$. In this case, the LM amplitude in Eq. (3) is also the sum,

$$\mathcal{F} = \mathcal{F}_0 + \mathcal{F}^{\mathrm{spin}}, \tag{8}$$

where the spin-independent LM amplitude is generated by the EDF in Eq. (6),

$$\mathcal{F}_0 = \frac{\delta^2 \mathcal{E}}{\delta \rho^2}. \tag{9}$$

Isotopic indices in Eqs. (1)–(9) are for brevity omitted.

The explicit expression for the L-phonon magnetic moment μ_L in magic nuclei corresponding to Fig. 1, with the short notation $|\nu_1\rangle = |1\rangle$, is as follows:

$$\mu_L = \sum_{123} (-1)^{L+1} \begin{pmatrix} 1 & L & L \\ 0 & L & -L \end{pmatrix} \begin{Bmatrix} 1 & L & L \\ j_3 & j_2 & j_1 \end{Bmatrix} \times \\ \times \langle 1|V(M1)|2\rangle \left[\langle 1|g_L|3\rangle \langle 3|\tilde{g}_L|2\rangle I_{123}^{GGG}(\omega_L) - \right. \\ \left. - \langle 1|\tilde{g}_L|3\rangle \langle 3|g_L|2\rangle I_{123}^{GGG}(-\omega_L) \right], \tag{10}$$

where

$$I_{123}^{GGG}(\omega_L) = \\ = \frac{1}{\varepsilon_2 - \varepsilon_1} \left[\frac{n_1(1-n_2)(1-n_3) - (1-n_1) n_2 n_3}{\varepsilon_1 - \varepsilon_3 - \omega_L} + \right. \\ \left. + \frac{n_1(1-n_2) n_3 - (1-n_1) n_2 (1-n_3)}{\varepsilon_2 - \varepsilon_3 - \omega_L} \right] + \\ + \frac{n_1 n_2 (1-n_3) - (1-n_1)(1-n_2) n_3}{(\varepsilon_1 - \varepsilon_3 - \omega_L)(\varepsilon_2 - \varepsilon_3 - \omega_L)}, \tag{11}$$

with

$$\tilde{g}_L(\omega) = g_L(-\omega) = g_{L0}(r;\omega)T_{LL0}(\mathbf{n},\alpha) - \\ - g_{L1}(r;\omega)T_{LL1}(\mathbf{n},\alpha). \quad (12)$$

In the ^{208}Pb nucleus several low-lying phonons are known with varying degree of collectivity. The lowest one, the 3^- phonon, possesses the highest collectivity whereas the strength of the 5^- mode is shared between two states. Let us first analyze the accuracy of describing the phonons themselves within our version of the self-consistent TFFS. Their characteristics are presented in Table 1. We see that the most collective 3^- level is described sufficiently well, 5_1^- and 5_2^- ones, a little worse. The properties of these two states depend crucially on the two lowest unperturbed ph-energies in the 5^- channel. The experimental values are $\Delta\varepsilon^n_{\rm exp}(g_{9/2}p^{-1}_{1/2}) = 3.43$ MeV and $\Delta\varepsilon^p_{\rm exp}(h_{9/2}s^{-1}_{1/2}) = 4.20$ MeV, i.e. the neutron component is the smaller one. The theoretical values derived from the DF3-a functional show the opposite behavior: $\Delta\varepsilon^n_{\rm th}(g_{9/2}p^{-1}_{1/2}) = 3.84$ MeV and $\Delta\varepsilon^p_{\rm th}(h_{9/2}s^{-1}_{1/2}) = 3.38$ MeV. This results in an inversion of our 5_1^- and 5_2^- states from the point of view of the weight of low-energy neutron and proton components, i.e. our 5_1^- state is mainly "proton" whereas the experimental one, "neutron", and vice versa for the 5_2^- state. This is not so important for the $B(E5)$ value, but, as we will see, inverses their magnetic properties.

The lowest 2_1^+ state and other states of positive parity are not very collective as there is no low-energy particle-hole configurations of positive parity except the spin-orbit doublets $(h^{-1}_{11/2}h_{9/2})$ for protons and $(i^{-1}_{13/2}i_{11/2})$ for neutrons. In such a situation, the theoretical values ω_L are close to the lowest particle-hole excitation energy, $\varepsilon_p(h_{9/2}) - \varepsilon_p(h_{11/2})$ or $\varepsilon_n(i_{11/2}) - \varepsilon_n(i_{13/2})$ in our case. The single-particle energies in ^{208}Pb we use which are generated with the DF3-a functional agree reasonably well on the average with the experimental ones [16]. Unfortunately the splitting of the two spin-orbit partners is some hundreds keV too large which is the main reason for the too high 2_1^+ phonon energy. Another reason for this discrepancy is evidently not taking into account the spin-orbit LM amplitude in Eq. (3) for the g_L vertex.

Let us now calculate magnetic moments and corresponding gyromagnetic ratios $g_L^{ph} = \mu_L^{ph}/L$ of the L-phonons in ^{208}Pb according Eq. (10). The results are given in Table 2. We showed separately the j- and s-components, according to Eq. (2), with the obvious substitution of $\mathbf{l} = \mathbf{j} - \mathbf{s}$. The subscripts n, p refer to the neutron and proton subsystems whereas L corresponds to their sum, e.g. $\mu_L^{(j)} = \mu_n^{(j)} + \mu_p^{(j)}$. Finally we get $\mu_L = \mu_L^{(j)} + \mu_L^{(s)}$. There are two experimental values of phonon gyromagnetic ratios, for the 3_1^- and 5_1^-. For the first one, our prediction reasonably agrees with the datum. For the 5_1^- state, in accordance with the above discussion, we put the calculation results found for the second theoretical 5^- state, the "neutron" one. In this case, again there is a reasonable agreement.

Table 1

Characteristics of the low-lying phonons in ^{208}Pb, ω_L (MeV) and $B(EL$, up)($e^2\cdot fm^{2L}$)

L^π	ω_L^{th}	$\omega_L^{\rm exp}$	$B(EL)^{th}$	$B(EL)^{\rm exp}$
3_1^-	2.684	2.615	$7.093\cdot10^5$	$6.12\cdot10^5$
5_1^-	3.353	3.198	$3.003\cdot10^8$	$4.47\cdot10^8$
5_2^-	3.787	3.708	$1.785\cdot10^8$	$2.41\cdot10^8$
2_1^+	4.747	4.086	$1.886\cdot10^3$	$3.18\cdot10^3$
2_2^+	5.004	4.928	$1.148\cdot10^3$	-
4_1^+	4.716	4.324	$3.007\cdot10^6$	-
4_2^+	5.367	4.911(?)	$8.462\cdot10^6$	-
6_1^+	4.735	-	$6.082\cdot10^9$	-
6_2^+	5.429	-	$1.744\cdot10^{10}$	-

To understand better the nature of the phonons we compare our theoretical g_L^{ph} values with the BM model prediction $g^{ph}_{L,\rm BM} = Z/A = 0.394$. We see that only for the 3^-- and 4_2^+-states our values are rather close to the BM one whereas in other cases there is nothing in common between these two theoretical predictions. Note that in the BM model the spin-component $\mu_L^{(s)}$ is absent. If we neglect in Eq. (10) the spin term of the effective field $V(M1)$ and put $\zeta_l = 0$, i.e. take $V(M1) = j$, we obtain the BM value of g_L^{ph} for all the states under consideration. Thus, the microscopic value of the gyromagnetic ratio deviates from the classic model prediction due to the spin term and non-zero value of ζ_l.

To check the formulas above and estimate the accuracy of the calculations, it is instructive to apply Eqs. (10), (11) to the spurious phonon $L^\pi = 1^-$, $\omega_{1^-} = 0$. In this case, the term g_{11} in the sum of Eq. (7) vanishes, whereas the term $g_{10}(\omega)$ is singular at $\omega = 0$ [6],

$$g_{10}(\omega) = \frac{1}{\sqrt{2\omega B_1}}\frac{\partial U}{\partial r}. \quad (13)$$

Here, $U(r)$ is the central part of the mean-field potential generated by the energy functional (6) and $B_1 = 3m/(4\pi A)$ is the BM mass coefficient [22]. Eq. (13) follows from the exact TFFS self-consistency relation [23] with some simplifications and neglecting the spin-orbit terms. The singularity in all the above expressions containing g_1^2 is compensated by the corresponding in-

Table 2

Magnetic moments (in μ_N units) of phonons in ^{208}Pb

L^π	$\mu_n^{(j)}$	$\mu_n^{(s)}$	μ_n	$\mu_p^{(j)}$	$\mu_p^{(s)}$	μ_p	$\mu_L^{(j)}$	$\mu_L^{(s)}$	μ_L	g_L^{ph}	$g_{L,\mathrm{exp}}^{ph}$ [1]
3^-	−0.074	−0.039	−0.113	1.566	0.058	1.492	1.492	0.019	1.511	0.463	0.63(7)
5_1^-	−0.215	−0.478	−0.693	0.853	−0.123	0.730	0.638	−0.600	0.037	0.008	0.022(8)
5_2^-	−0.027	−0.018	-0.046	4.733	0.278	5.011	4.705	0.260	4.965	0.993	
2_1^+	−0.027	0.000	−0.027	1.536	0.493	2.029	1.509	0.492	2.002	1.001	
2_2^+	−0.027	0.004	−0.022	1.541	0.406	1.947	1.514	0.411	1.925	0.962	
4_1^+	−0.009	−0.010	−0.018	4.017	0.449	4.466	4.008	0.440	4.448	1.112	
4_2^+	−0.112	−0.232	−0.343	1.822	0.276	2.098	1.711	0.044	1.755	0.439	
6_1^+	−0.005	−0.004	−0.009	6.172	0.294	6.466	6.167	0.290	6.457	1.076	
6_2^+	−0.075	−0.147	−0.222	4.765	0.092	4.857	4.690	−0.054	4.636	0.773	

tegrals of the Green functions which are proportional to ω. This approximation for g_1 violates a little the normalization relation (4) leading to the value -1.074 instead of -1. If we correct the normalization, we obtain for the magnetic moment of the spurious 1^--phonon we obtain $\mu(1^-) = 0.403$ in good agreement with the BM gyromagnetic ratio 0.394. This calculation confirms the self-consistency of the scheme developed above.

In our calculations, the spin component is negligible for the 3^--state only. It confirms that this state, indeed, is most similar to the BM surface vibrations. The phonon creation amplitudes g_L are displayed in Figs. 2–4 for the states 3^-, 2_1^+, and 5_1^-, respectively. All of

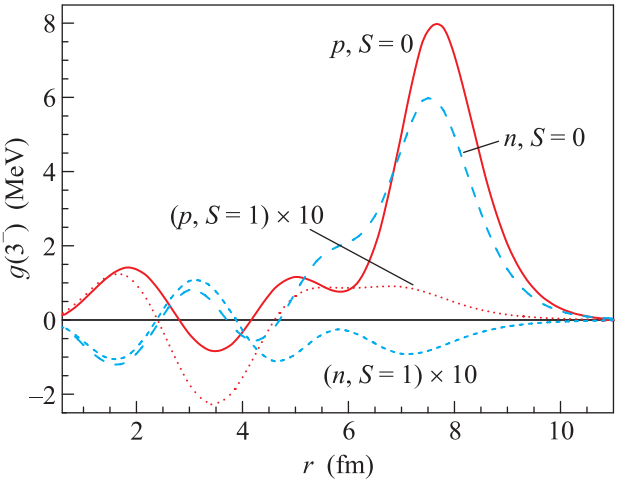

Fig. 2. (Color online) Components of the vertex g_L, $L^\pi = 3^-$, in ^{208}Pb

them show the BM-like ($\propto \partial U/\partial r$) surface maxima of the spin-zero components which are significantly larger than components with $S = 1$. However, for 5_1^- and 2_1^+ states the spin components are not negligible. Moreover, they possess maxima at $r \simeq 6$ fm where the wave functions of the single-particle states in vicinity of Fermi

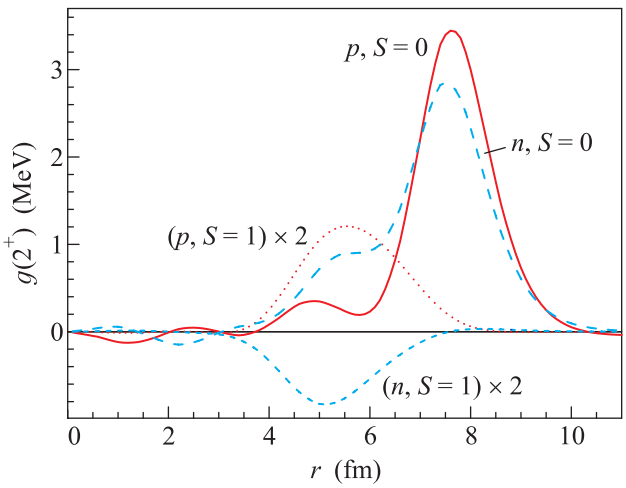

Fig. 3. (Color online) Components of the vertex g_L, $L^\pi = 2_1^+$, in ^{208}Pb

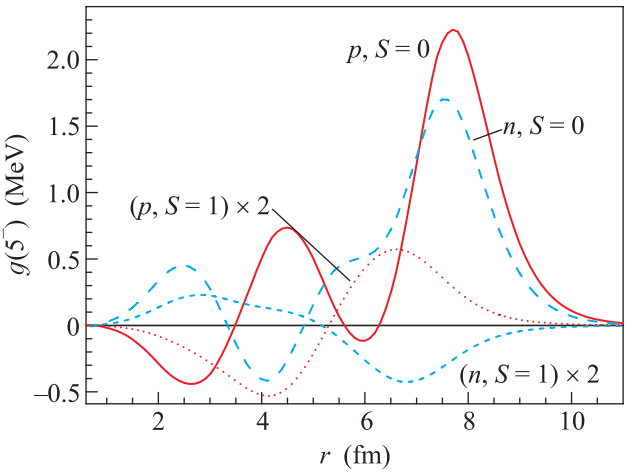

Fig. 4. (Color online) Components of the vertex g_L, $L^\pi = 5_1^-$, in ^{208}Pb

surface have their maxima too. This is true for pairs of the radial wave functions $\{R_\nu(r)R_{\nu'}(r)\}$ which cor-

respond to the term with a small energy denominator in Eq. (11) which always exists for the phonon states under discussion. At the same time the maxima of the main, $S = 0$, components are shifted to the right by $\simeq (1-2)$ fm due to the coherent contribution of many high-lying *ph*-components. However, in this region the wave functions under discussion are small. As a result, for these states the contribution of the $S = 1$ to the phonon magnetic moment is often rather big. This is the main reason why the self-consistent TFFS g_L^{ph} values differ from the BM ones significantly for all phonons which collectivity is not sufficiently high. The exception for the 4_2^+ phonon is occasional. For this state, as it is seen from Table 2, the terms $\mu_n^{(s)}$ and $\mu_p^{(s)}$ cancel each other almost completely.

To summarize, in the magic ^{208}Pb nucleus, the gyromagnetic ratio g_L^{ph} for the lowest 3^- phonon is very close the BM model prediction $g_{L,\mathrm{BM}}^{ph} = Z/A$. This state is the most collective one in ^{208}Pb. All other phonons which we have considered are much less collective and their g_L^{ph} values deviate significantly from the BM predictions due to the strong spin contributions to the phonon creation vertex g_L.

Generalization of the theory developed above for non-magic nuclei where pairing is important is rather complicated. Seven additional triangles appear similar to the one in Fig. 1. It occurs, first, because the 3-vector $\hat{g}_L$ with one normal and two anomalous components appears in this case instead one vertex (3) [4, 12]. As it is demonstrated in Figs. 5 and 6 for the collective 2_1^+ state

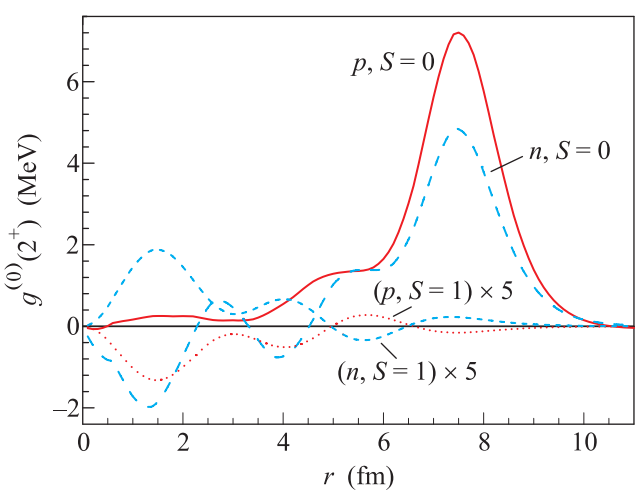

Fig. 5. (Color online) Components of the normal amplitude $g_2^{(0)}$ in ^{200}Pb

in the non-magic nucleus ^{200}Pb, the anomalous component $g_n^{(1)}(2_1^+)$ is comparable with the normal neutron vertex $g_n^{(0)}(2_1^+)$. Although, see Fig. 5, the spin compo-

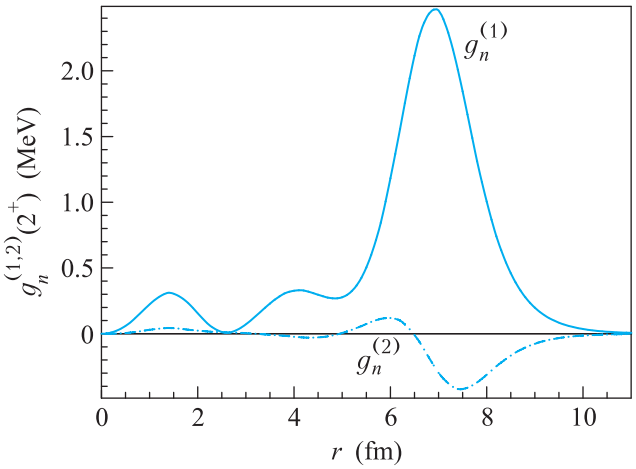

Fig. 6. (Color online) Components of the neutron anomalous amplitudes $g_2^{(1)}$ and $g_2^{(2)}$ in ^{200}Pb

nents of the normal vertices $g_{n,p}^{(1)}(2_1^+)$ are small, just as for the collective 3^- state in ^{208}Pb, the contributions of the anomalous components can also result in deviations from the BM model predictions. Second, in superfluid nuclei, instead of one propagator A one deals with the $3 \otimes 3$ propagator matrix $\hat{A}$ containing the energy integrals of different products of the Green function $G(\varepsilon)$ and the two Gorkov functions $F^{(1,2)}(\varepsilon)$ [4, 12]. Such a generalization is in a progress.

The work was partly supported by the DFG and RFBR Grants #436RUS113/994/0-1 and 09-02-91352NNIO-a, by the Grant NSh-215.2012.2 of the Russian Ministry for Science and Education, and by the RFBR Grants 11-02-00467-a, 12-02-00955-a, 13-02-00085-a, and 13-02-12106. We thank O.I. Achakovskiy and N.V. Gnezdilov for help. Three of us, E.S., S.Ka., and S.T., are grateful to the Institut für Kernphysik, Forschungszentrum Jülich for its hospitality.

1. N. J. Stone, Atomic Data Nuclear Data Table **90**, 75 (2005).
2. P. Vingerhoets, K. T. Flanagan, M. Avgoulea et al., Phys. Rev. C **82**, 064311 (2010).
3. M. Honma, T. Otsuka, B. A. Brown, and T. Mizusaki, Phys. Rev. C **69**, 034335 (2004).
4. A. B. Migdal, *Theory of finite Fermi systems and applications to atomic nuclei*, Nauka, Moscow, 1965 [Wiley, N.Y., 1967].
5. A. B. Migdal, *Theory of finite Fermi systems and applications to atomic nuclei*, 2-nd ed., Nauka, Moscow, 1983.
6. V. A. Khodel and E. E. Saperstein, Phys. Rep. **92**, 183 (1982).
7. I. N. Borzov, E. E. Saperstein, and S. V. Tolokonnikov, Phys. At. Nucl. **71**, 469 (2008).

8. I. N. Borzov, E. E. Saperstein, S. V. Tolokonnikov et al., Eur. Phys. J. A **45**, 159 (2010).
9. S. V. Tolokonnikov, S. Kamerdzhiev, D. Voytenkov et al., Phys. Rev. C **84**, 064324 (2011).
10. S. V. Tolokonnikov, S. Kamerdzhiev, S. Krewald et al., EPJA **48**, 70 (2012).
11. S. Kamerdzhiev, S. Krewald, S. V. Tolokonnikov et al., EPJ Web of Conferences **38**, 10002 (2012).
12. D. Voitenkov, S. Kamerdzhiev, S. Krewald et al., PRC **85**, 054319 (2012).
13. A. V. Smirnov, S. V. Tolokonnikov, and S. A. Fayans, Sov. J. Nucl. Phys. **48**, 995 (1988).
14. S. A. Fayans, JETP Lett. **68**, 169 (1998).
15. S. A. Fayans, S. V. Tolokonnikov, E. L. Trykov, and D. Zawischa, Nucl. Phys. A **676**, 49 (2000).
16. S. V. Tolokonnikov and E. E. Saperstein, Phys. Atom. Nucl. **73**, 1684 (2010).
17. S. V. Tolokonnikov, S. Kamerdzhiev, S. Krewald et al., EPJ Web of Conferences **38**, 04002 (2012).
18. E. E. Saperstein, O. Achakovskiy, S. Kamerdzhiev et al., arXiv:1305.1123[nucl-th] (2013).
19. E. E. Saperstein, S. Kamerdzhiev, S. Krewald et al., EPL, to be published.
20. A. Bohr and B. R. Mottelson, *Nuclear Structure*, Benjamin, N.Y., Amsterdam, 1974, v. 2.
21. I. Hamamoto, Phys. Lett. B **61**, 343 (1973).
22. A. Bohr and B. R. Mottelson, *Nuclear Structure*, Benjamin, N.Y., Amsterdam, 1969, v. 1.
23. S. A. Fayans and V. A. Khodel, JETP Lett. **17**, 444 (1973).